Journal of Engineering Physics and Thermophysics, Vol. 73, No. 5, 2000

MAGNETIC FIELD EFFECTS ON MIXED CONVECTION BETWEEN ROTATING COAXIAL DISKS

M. F. Dimian[a] and A. H. Essawy[b]

UDC 532.135

This paper deals with a similarity analysis of axisymmetric mixed convection between two horizontal infinite rotating coaxial disks in the presence of a magnetic field. The governing Navier–Stokes equations and energy equation reduce to a set of nonlinear ordinary differential equations using similarity. The resulting set of ordinary differential equations has been solved numerically using a shooting method and is represented graphically. For Reynolds number, Re, up to 500 and buoyancy parameter, $B = \beta\Delta T$, of the range $|B| \le 0.05$, the flow and heat transfer characteristics with Prandtl numbers 7, 0.7, 0.1 and 0.01 and magnetic field parameters of m = 0.5, 1, and 2 are examined. The heat transfer increases with the Prandtl number but decreases with the magnetic parameter. It is established that the rotation of the two disks has a very small effect on the temperature of the fluid and the heat-transfer process.

Introduction. Fluid flow and transfer associated with a rotating disk system are of academic and practical interest for the wide applications of rotating machinery. Due to the rotation of the disks, two rotational forces, Coriolis and centrifugal, are present in the flow field. By considering the fluid density variation and invoking the Boussinesq approximation, the so-called centrifugal buoyancy can be taken into account. The buoyancy effects on steady transport phenomena in rotating disk systems have been studied by Soong [7-9].

The present study extends the work of Soong [7] to magnetic field effects on nonisothermal flow and heat transfer between horizontal infinite rotating coaxial disks by using a similarity model for rotation mixed convection and the magnetic field. The flow of an electrically conducting incompressible fluid in the presence of a magnetic field has been analyzed by El-Shekh et al. [3], Hamza [4], and Kumari et al. [5, 6] for flow between parallel disks.

The governing Navier–Stokes equations and the energy equation with a rotating frame of reference are formulated, and the Boussinesq approximation is invoked to explore centrifugal buoyancy effects.

Co-rotating disks ($\Omega_2 = \Omega_1$) and a rotating system ($\Omega_1 \neq \Omega_2 = 0$) are considered to investigate the free and mixed convection flows, respectively, in the presence of a magnetic field. A transformation which reduces the Navier–Stokes equations and energy equation to a set of nonlinear ordinary differential equations was described by Soong [7] and Ibrahim [2]. The resulting set of nonlinear ordinary differential equations has been solved numerically using a shooting method.

2. Problem Statement and Formulation. Consider the axisymmetric steady flow of a viscous incompressible fluid contained between two horizontal parallel infinite disks and separated by a spacing S. The disks lie at constant temperatures T_1 and T_2, and rotate with rotational speeds Ω_1 and Ω_2, respectively, as shown in Fig. 1. Cylindrical coordinates (R, ϕ, z) are fixed on the lower disk and their origin lies at the disk center. With respect to the rotating frame of reference, Coriolis and centrifugal forces appear explicitly in the momentum equation. The fluid flow is assumed to be steady, laminar, axisymmetric and of constant properties, and the Boussinesq approximation is invoked for study of the centrifugal buoyancy effects.

[a]Department of Mathematics, Faculty of Science, Ain Shams University, Cairo, Egypt; [b]Department of Mathematics, Faculty of Science, El-minia University, El-minia, Egypt. Published in Inzhenerno-Fizicheskii Zhurnal, Vol. 73, No. 5, pp. 1109-1117, September–October, 2000. Original article submitted May 27, 1999.

 1062-0125/00/7305-1082$25.00

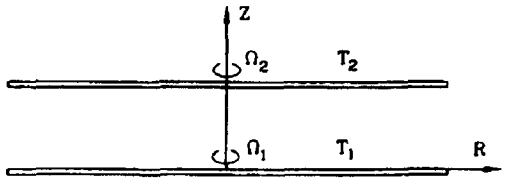

Fig. 1. Physical model of two co-axially rotating infinite disks.

A magnetic field of strength M is applied normal to the disk surface, and it is assumed that the magnetic Reynolds number is small. Hence the induced magnetic field can be neglected as compared to the applied magnetic field.

The velocity components in the R, Φ and z directions are u, v and w, respectively. Considering the laminar density temperature relation $\rho = \rho_r[1 - \beta(T - T_r)]$, the governing equations can be depicted as:

Navier–Stokes equations

$$u\frac{\partial u}{\partial R} - \frac{v^2}{R} + w\frac{\partial u}{\partial z} - 2\Omega_1 [1 - \beta (T - T_r)]\, v + \Omega_1 R\beta (T - T_r) =$$

$$-\frac{1}{\rho_r}\frac{\partial P'}{\partial R} + \nu\left[\frac{1}{R}\frac{\partial}{\partial R}\left(R\frac{\partial u}{\partial R}\right) + \frac{\partial^2 u}{\partial z^2}\right] - \frac{\sigma F^2}{\rho_r} u\,, \tag{1}$$

$$u\frac{\partial v}{\partial R} + \frac{uv}{R} + w\frac{\partial v}{\partial z} + 2\Omega_1 [1 - \beta (T - T_r)]u =$$

$$\nu\left[\frac{1}{R}\frac{\partial}{\partial R}\left(R\frac{\partial v}{\partial R}\right) + \frac{\partial^2 v}{\partial z^2} - \frac{v}{R^2}\right] - \frac{\sigma F^2}{\rho_r} v\,, \tag{2}$$

continuity equation,

$$\frac{\partial}{\partial R}(Ru) + R\frac{\partial}{\partial z}(w) = 0\,, \tag{3}$$

energy equation,

$$(\underline{v} \cdot \nabla)\, T = \alpha \nabla^2 T\,. \tag{4}$$

Here, $P' = P - P_r$ is the pressure departure from the reference condition. Equations (1)-(4) governing the axisymmetric steady flow without a magnetic field ($F \neq 0$) are the same as those studied by Soong [7]. By using the dimensionless variables and parameters

$$u(R, z) = \frac{-R\Omega_1 H'(\eta)}{2\sqrt{\mathrm{Re}}}\,,\quad v(R, z) = R\Omega_1 G(\eta)\,,\quad w(R, z) = \sqrt{\nu\Omega_1}\, H(\eta)$$

$$T - T_r = \theta(\eta)\nabla T\,,\quad \eta = \frac{z}{S}\,,\quad \mathrm{Re} = \frac{\Omega_1 S^2}{\nu} \tag{5}$$

where ρ, ν, and σ are, respectively, density, kinematic viscosity, and electrical conductivity, $\Delta T = T_2 - T_1$ is the characteristic temperature difference, and η is the similarity variable, Eqs. (1)-(4) can be recast into the following dimensionless form:

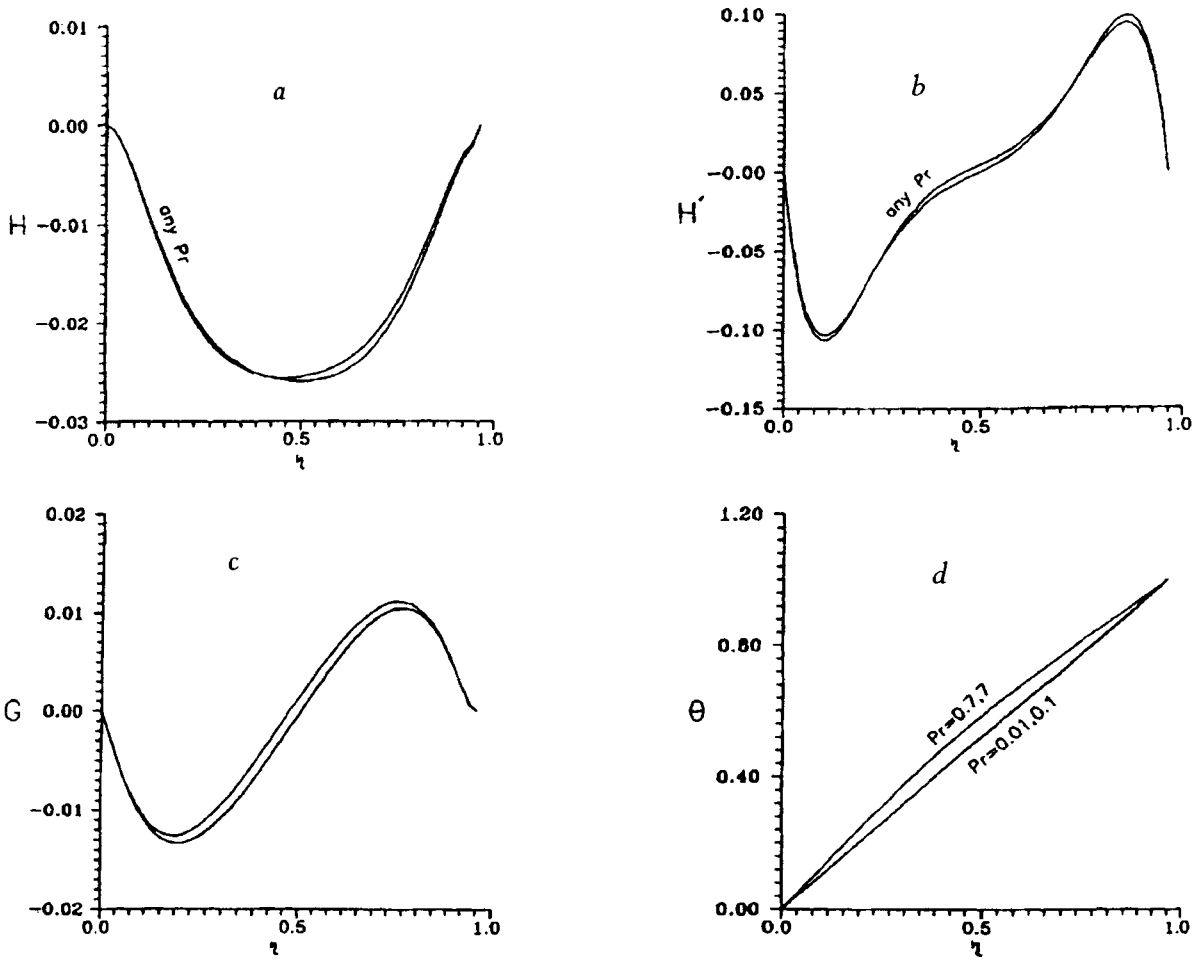

Fig. 2. Distribution of axial flow velocity (a), radiation flow velocity (b), tangential flow velocity (c), and temperature (d): Re = 50, B = 0.05, M = 1, Pr = 0.01, 0.1, 0.7, 7; γ = 0.

$$H''' = \sqrt{\mathrm{Re}}\, HH''' + 4\mathrm{Re}^{3/2}\,[(1+G)\,G' - B\,(G'\theta + G\theta')] -$$

$$- B\mathrm{Re}^{3/2}\,\theta' + \mathrm{Re}^2 MH'', \tag{6}$$

$$G'' = \sqrt{\mathrm{Re}}\,[HG' - H'\,(1+G) + BH'\theta] + MG, \tag{7}$$

$$\theta'' = \mathrm{Pr}\sqrt{\mathrm{Re}}\, H\theta', \tag{8}$$

with

$$M = \frac{\sigma F^2}{\rho_f \Omega_1 \mathrm{Re}} \tag{9}$$

where G, H, and θ are the tangential and axial velocities and the temperature function, respectively. The parameter Pr is the Prandtl number, and Pr = 0.7 for air is used in the present study. The rotational effect is characterized by the Reynolds number, Re; its range is from 50 to 500.

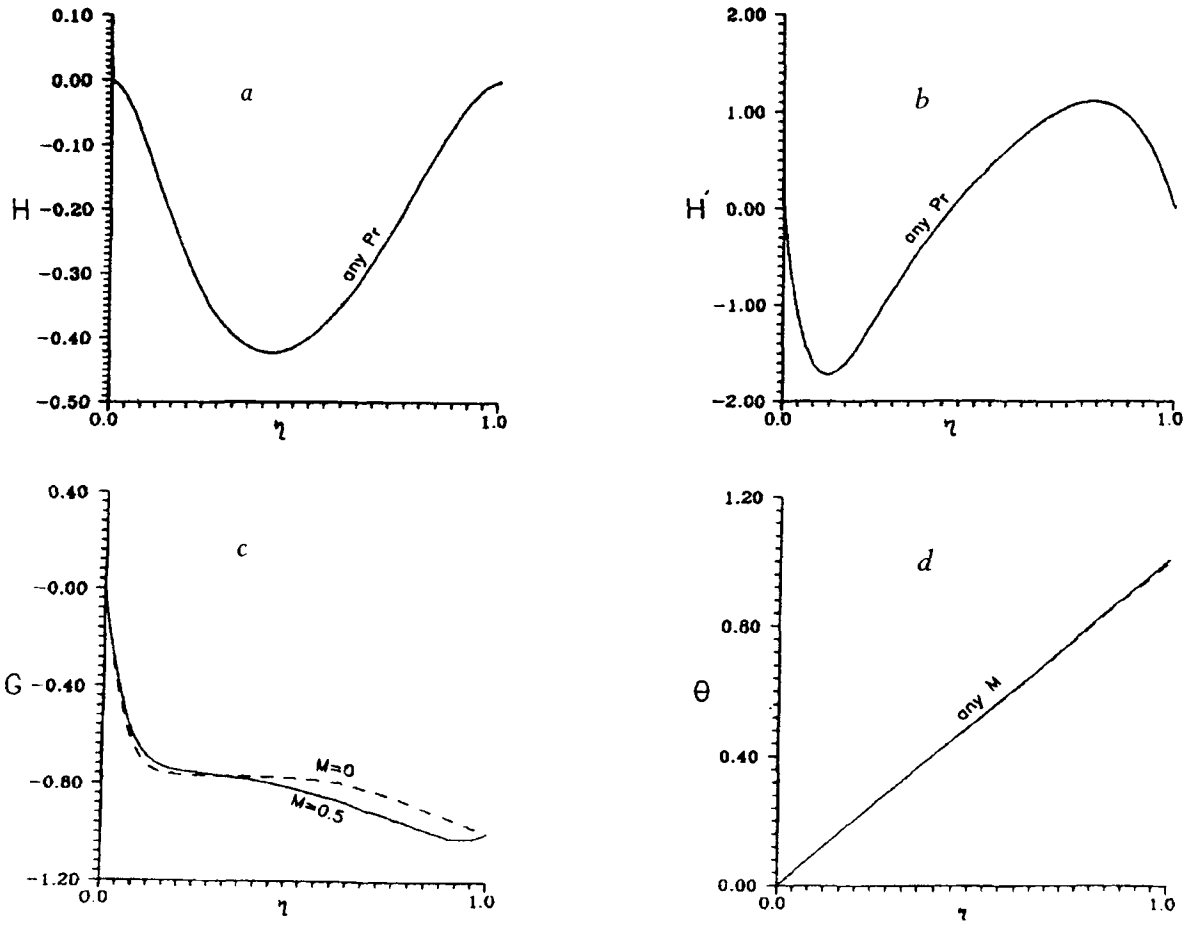

Fig. 3. Distribution of axial flow velocity (a) [Re = 50; B = 0; M = 1; Pr = 0.01, 0.1, 0.7, 7; γ = −1], radiation flow velocity (b) [Re = 50, B = 0, M = 1, Pr = 0.01, 0.1, 0.7, 7; γ = −1], tangential flow velcoity (c) [Re = 500; B = 0.05; M = 0.5; Pr = 0.01; γ = −1], and temperature (d) [Re = 500; B = 0.05; M = 0, 0.5; Pr = 0.01; γ = −1].

The boundary conditions for the velocity and temperature functions are

$$\left.\begin{aligned} H(0) = H'(0) = H(1) = H'(1) = 0 \\ G(0) = G(1) - \gamma = 0 \\ \theta(0) = \theta(1) - 1 = 0 \end{aligned}\right\}, \tag{10}$$

where the parameter $\theta = \dfrac{\Omega_2 - \Omega_1}{\Omega_1}$ denotes the dimensionless rotation rate of the upper disk.

3. Governing Parameters. Five parameters are involved in the problem; they are Pr, Re, B, θ and R. The Prandtl number indicates the relative importance of the viscous-to-thermal diffusion effect, $\mathrm{Pr} = \dfrac{\nu}{\alpha}$. The rotational Reynolds number $\mathrm{Re} = \dfrac{\Omega_1 S^2}{\nu}$ (S is the spacing between the two coaxial disks) represents the ratio between the angular velocity of the lower disk and the kinematic viscosity of the fluid. When Re increases, this

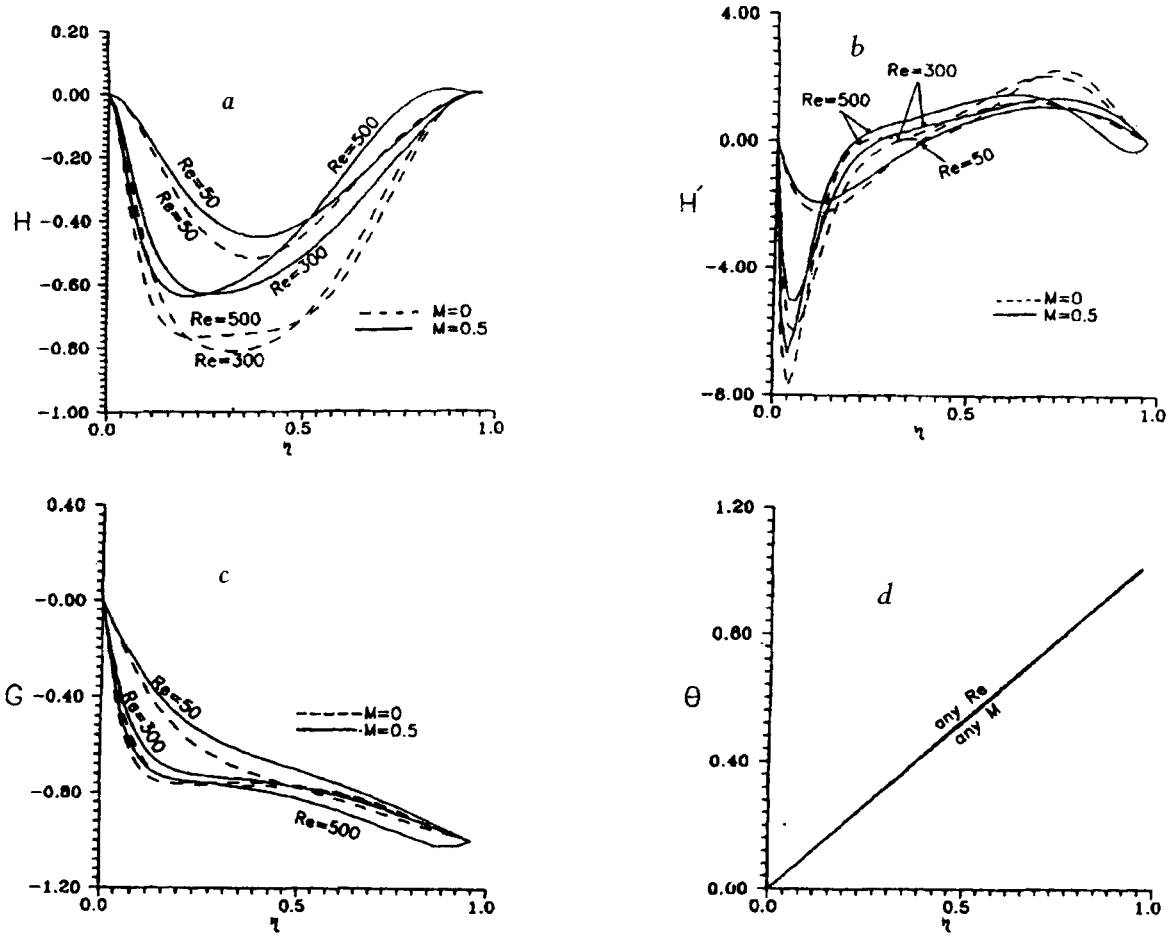

Fig. 4. Distribution of axial flow velocity (a), radial flow velocity (b), tangential flow velocity (c), and temperature (d): Re = 50, 300, 500, B = 0.05, M = 0, 0.5; Pr = 0.01; $\gamma = -1$.

means that either the angular velocity of the lower disk increases or the kinematic viscosity of the fluid decreases. The thermal Rossby number B measures the buoyancy effect. The parameter θ denotes the relative rotation rate of the upper disk with respect to that of the lower disk. For example, the values of $\gamma = 0$ and $\gamma = -1$ correspond to the cases of co-rotating disks ($\Omega_1 = \Omega_2$) and rotor-stator ($\Omega_1 \neq \Omega_2 = 0$), respectively. Note that, in this two-disk flow configuration the cases of $\gamma = 0$ and $B \neq 0$ are pure free convection ($B = \beta(T_2 - T_1)$), while forced convection is characterized by $\gamma \neq 0$ and $B = 0$. For a nonzero B as well as γ, the problem becomes a mixed convection one, in which Re can be used to characterize the forced flow effect. In the conventional free-convection study, for the validity of the Boussinesq approximation, $\beta\Delta T$ was usually small, for example, less than 0.05 in the study of Soong [7].

A positive value of B implies $T_1 < T_2$, the temperature of the fluid adjacent to the lower disk is higher than T_1 and the flow is designated as a buoyancy-opposed flow. Conversely, the flow with $B < 0$ (or $T_1 > T_2$) is a buoyancy-assisted one. The magnetic number M characterizes the magnetic effect.

4. Numerical Procedure. To solve the coupled point boundary value problem expressed by Eqs. (6)-(8) subject to the boundary conditions (10) for all values of η, which is the similarity variable, we apply the fourth-order Runge–Kutta integration scheme with the Nachtsheim–Swigert shooting technique [1].

These equations can be expressed as

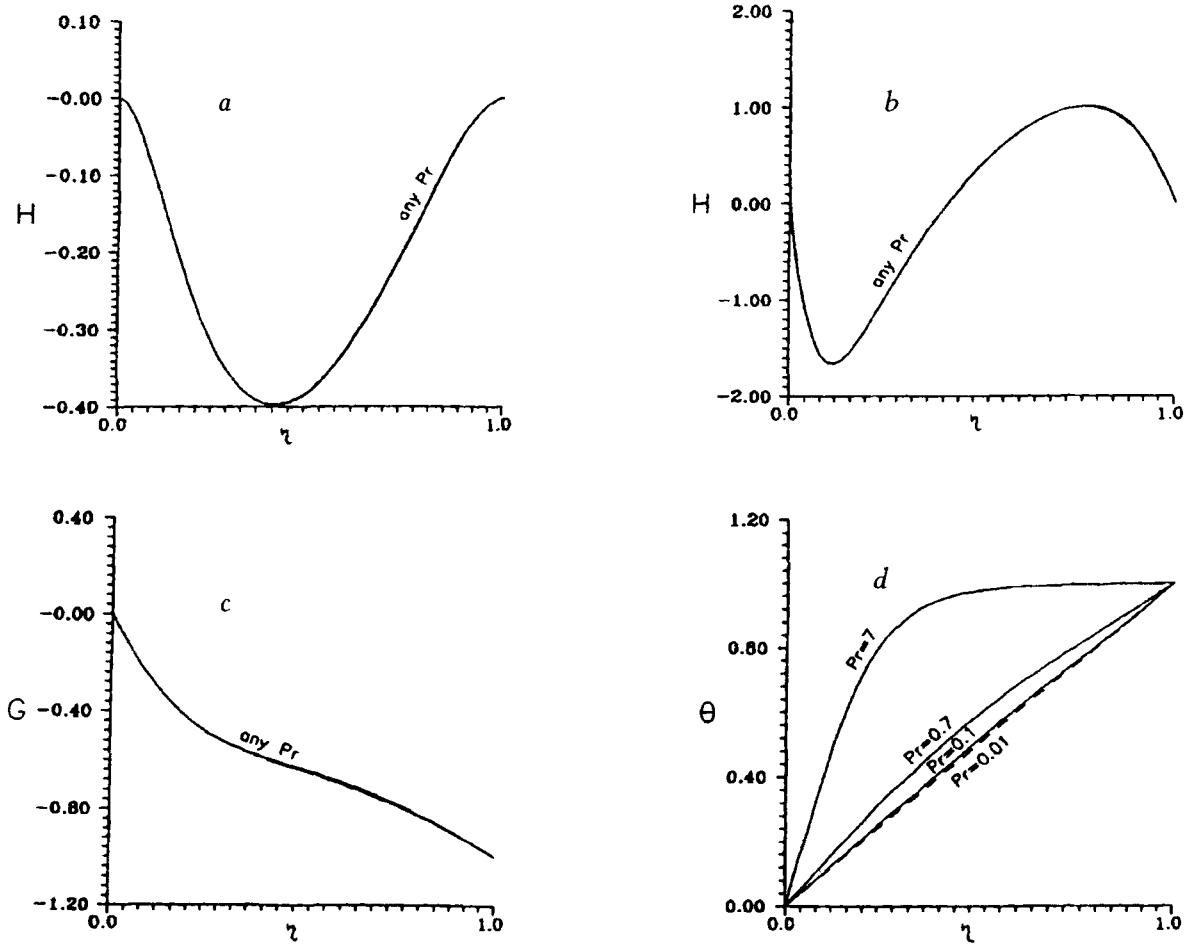

Fig. 5. Distribution of axial flow velocity (a), radial flow velocity (b), tangential flow velocity (c), and temperature (d): Re = 50, B = 0.05, M = 1, Pr = 0.01, 0.1, 0.7, 7; $\gamma = -1$.

$$\frac{dy_i}{d\eta} = f_i(\eta, y_1, y_2, ..., y_n), \quad i = 1, 2, ..., N. \tag{11}$$

A typical shooting method can be started with the guessed missing conditions:

$$H'' = a, \quad H'''(0) = b, \quad G'(0) = c \quad \text{and} \quad \theta'(0) = d. \tag{12}$$

In an iterative procedure, the values of a, b, c, and d are updated continuously using Newton's method until the boundary conditions at η = 1, i.e.,

$$H(1) = H'(1) = G(1) - \gamma = \theta(1) - 1 = 0 \tag{13}$$

are met. The iteration is regarded as convergent if the stopping criterion

$$\max(\Delta a, \Delta b, \Delta c, \Delta d) \leq 10^{-6} \tag{14}$$

is satisfied.

Low Re and M solutions are easily obtained using conventional shooting techniques. However, due to the stiffness of the system, the convergent solution is difficult.

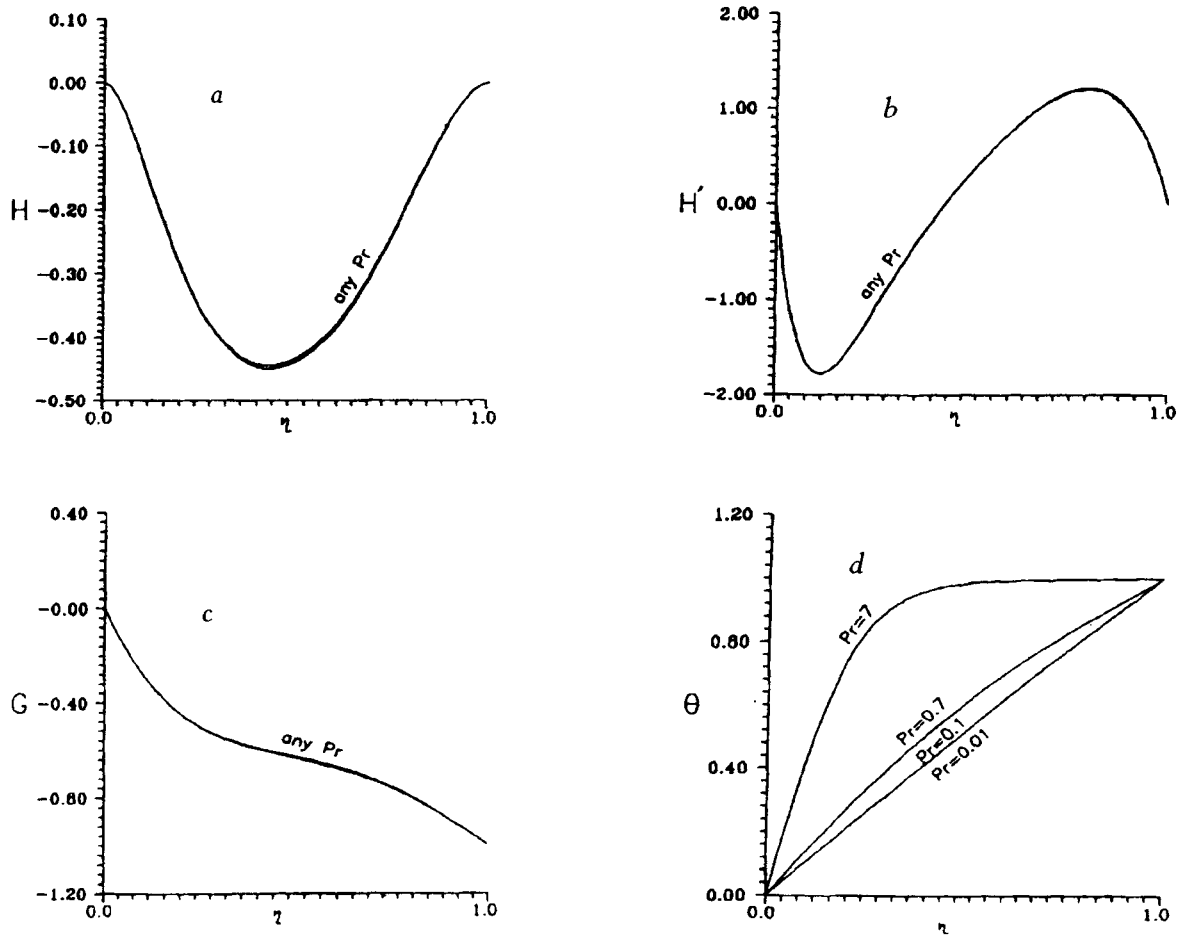

Fig. 6. Distribution of axial flow velocity (a), radial flow velocity (b), tangential flow velocity (c), and temperature (d): Re = 50, B = –0.05, M = 1, Pr = 0.01, 0.1, 0.7, 7; γ = –1.

5. Results and Discussion. Rotation-induced buoyancy effects were studied by Soong [3], while in the present work the emphasis is placed on rotation-induced buoyancy effects in presence of a magnetic field. Figure 2 shows the free-convection solutions for Re = 50, M = 1, γ = 0 and B = 0.05, ($T_2 > T_1$). For higher Pr, e.g., Pr = 7, the temperature distribution deviations from the conductive solutions are due to the convection effect. For an increasing temperature gradient near the lower disk, the cooler fluid is accelerated radically outward. This enhances the peak value of the radial velocity, which, in turn, alters the axial velocity distribution H and through the action of the Coriolis buoyancy effect the circumferential velocity G presents a noticeable change.

Forced convection (buoyancy free) solutions for a rotor-stator system (γ = –1) with Re = 50, M = 1, B = 0 ($T_1 = T_2$) and variable Prandtl number are presented in Fig. 3. Since the velocity-temperature coupling has been broken by ignoring the buoyancy effect, the velocity profiles become independent of the Prandtl number, while the temperature solutions are still a strong function of Pr. For relatively high Prandtl numbers, e.g., Pr = 0.7 and 7 in Fig. 3, a thermal buoyancy layer emerges on the lower disk. The appearance of the thermal buoyancy layer is attributed to the relatively strong convection effect.

Figures 5 and 6 show the buoyancy-influenced counterparts of the case in Fig. 3. In Fig. 5 with B = 0.05 ($T_2 > T_1$) and the Prandtl number Pr = 7, the temperature function changes abruptly in the thin thermal boundary layer but remains uniform in a large portion of the wheel space. As Pr decreases from 7 to 0.01, the thermal diffusion becomes more and more important, and then the temperature variation appears notably in the

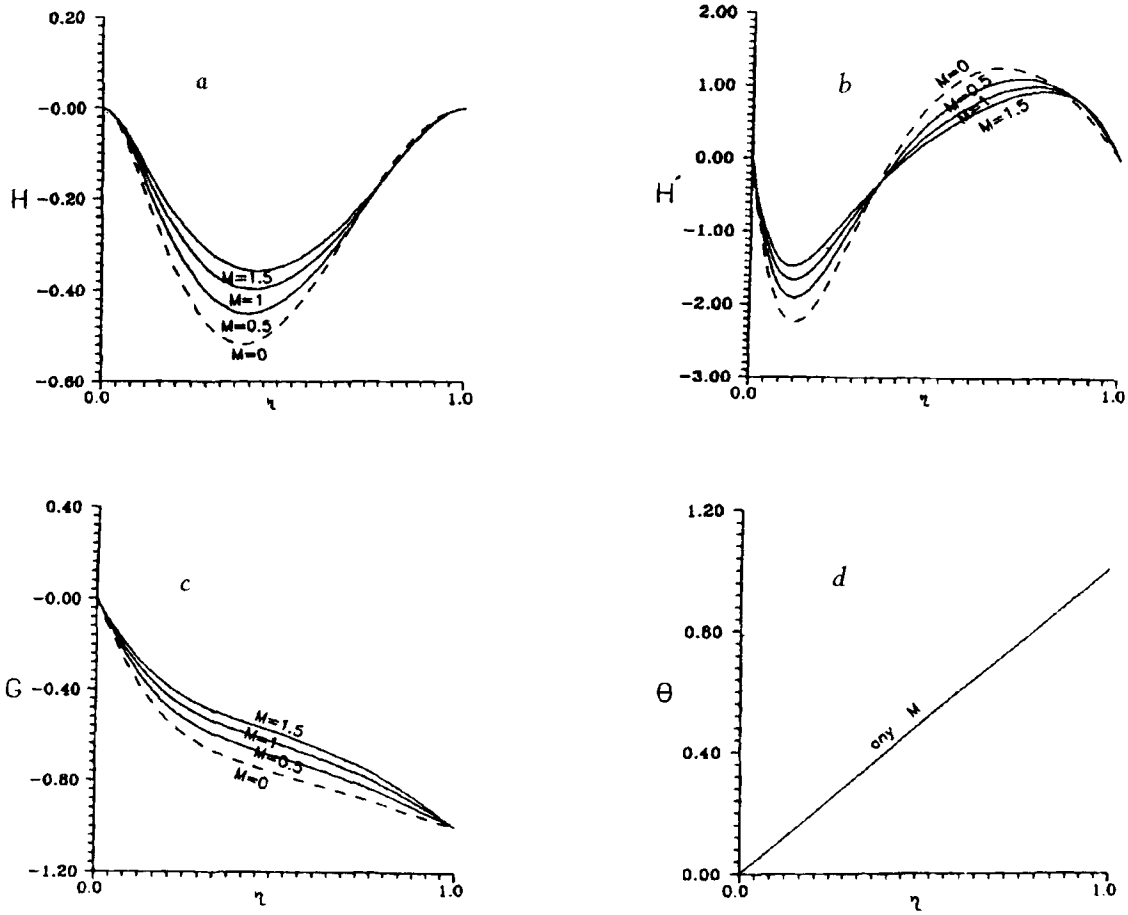

Fig. 7. Distribution of axial flow velocity (a), radial flow velocity (b), tangential flow velocity (c), and temperature (d): Re = 50, B = 0.05, M = 0, 0.5, 1, 1.5, Pr = 0.01; $\gamma = -1$.

whole domain rather than confined in a narrow region of the thermal boundary layer. For small Pr, the temperature gradient near the lower disk, i.e., $z = 0$, is alleviated. Therefore, the reduction in the buoyancy-opposing effect enhances the radial velocity peak near the lower disk. The axial velocity distribution is modified with variation of the radial velocity. Due to coupling of the Coriolis-induced buoyancy in circumferential fluid motion and the Prandtl number effects, a salient Pr-dependence of the circumferential velocity is present. In the case of buoyancy-assisted flow with $B = -0.05$ ($T_2 < T_1$) the velocity field is only slightly altered by the change in Prandtl number (Fig. 6), although the temperature distribution varies as in buoyancy-free and buoyancy-opposed flows.

Figures 4, 7, and 8 show that the velocity components decrease with an increase in the magnetic field while temperature distribution is independent of the magnetic field. Figure 4 shows that the temperature distribution is independent of the Reynolds number, Re, while the velocity profiles are strange functions of Re; an increase in Re gives an increase in the magnitude of the velocity components.

It is established that the rotation of the two disks has a very small effect on the fluid temperature and the heat-transfer process. The effect of the Prandtl number in the presence of a magnetic field on the velocity components and temperature distribution is small compared with that without a magnetic field.

The results are found to be in very good agreement, especially when $M = 0$, with those of Soong [7]. When Re increases, this means that either the angular velocity of the lower disk increases or the kinematic viscosity of the fluid decreases.

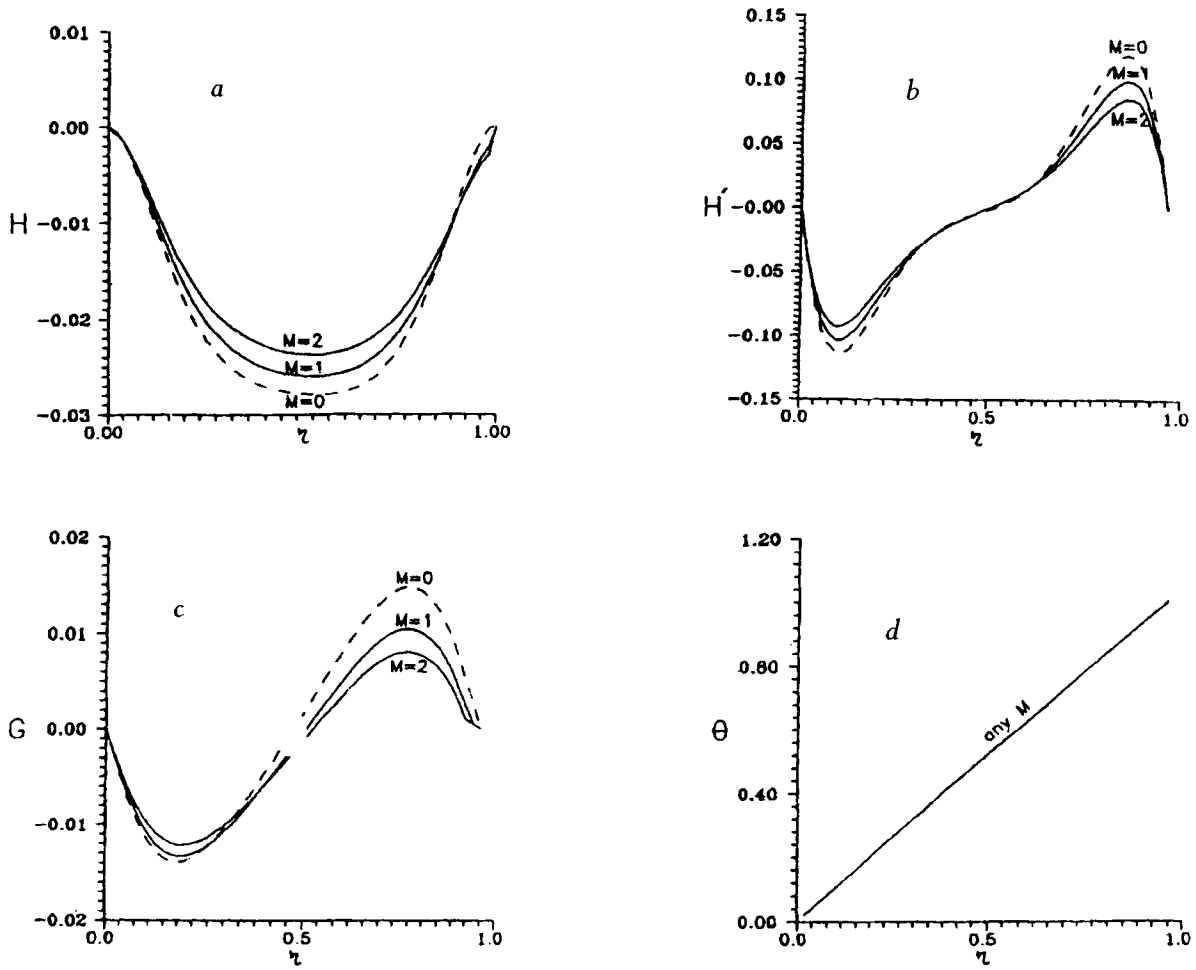

Fig. 8. Distribution of axial flow velocity (a), radial flow velocity (b), tangential flow velocity (c), and temperature (d): Re = 50, B = 0.05, M = 0, 1, 2, Pr = 0.01; γ = 0.

6. Concluding Remarks. The Prandtl number effects on buoyancy-influenced nonisothermal flow between coaxial disks have been studied by using a similarity model. The results reveal that a change in Pr leads to a variation of the temperature distribution, which, in turn, modifies the velocity field by rotation-induced buoyancy effects. From the present theoretical analysis, it can be disclosed that for two-disk problems the Prandtl number has a significant impact on the flow and heat-transfer characteristics in either free convection or mixed convection. In the typical cases of mixed-convection flow and heat transfer with the same measure of buoyancy, $|B|$ = 0.05, the Pr effect of buoyancy-opposed flow (B = 0.05 ($T_2 > T_1$)) is more pronounced than that in buoyancy-assisted ones (B = −0.05 ($T_2 < T_1$)). The heat transfer increases with the Prandtl number but decreases with the magnetic parameter. It is established that the rotation of the two disks has a very small effect on the temperature of the fluid and the heat-transfer process.

NOTATION

T_1, temperature of lower disk; T_2, temperature of upper disk; Ω_1, rotational speed of lower disk; Ω_2, rotational speed of upper disk; (R, ϕ, z), cylindrical coordinates; (u, v, w), velocity components; M, strength of magnetic field; ρ, density of fluid; ν, kinematic viscosity; σ, electrical conductivity; η, similarity variable; (G,

H), tangential and axial velocities; θ, temperature function; Pr, Prandtl number, $\mathrm{Pr} = \frac{\nu}{a}$; Re, Reynolds number, $\mathrm{Re} = \frac{\Omega_1 S^2}{\nu}$; S, spacing between two coaxial disks; B, thermal Rossby number, which measures the buoyancy effect, $B = \beta(T_2 - T_1)$; γ, dimensionless rotation velocity of upper disk, $\gamma = \frac{\Omega_2 - \Omega_1}{\Omega_1}$.

REFERENCES

1. J. A. Adams and D. F. Rogers, in: *Computer-Aided Heat Transfer Analysis*, McGraw-Hill, Tokyo (1973), p. 285.
2. S. S. Elshekh, M. K. Abd El Hady, and F. N. Ibrahim, *Int. Eng. Sci.*, **34**, No. 10, 1183-1195 (1996).
3. F. N. Ibrahim, *J. Phys. D, Appl. Phys.*, **24**, 1293-1299 (1991).
4. E. A. Hamza, *J. Phys. D, Appl. Phys.*, **24**, 547-554 (1991).
5. M. Kumari, H. S. Takhar, and G. Nath, *Int. J. Eng. Sci.*, **31**, No. 12, 1659-1668 (1993).
6. M. Kumari, H. S. Takhar, and G. Nath, *Int. J. Eng. Sci.*, **33**, No. 6, 781-791 (1995).
7. C. Y. Soong, *Int. J. Rotating Machinery*, **2**, No. 3, 161-166 (1995).
8. C. Y. Soong, *Int. J. Mass Transfer*, **39**, No. 8, 1569-1583 (1996).
9. C. Y. Soong, *Int. J. Heat Transfer*, **18**, No. 10, 1865-1878 (1995).